SRTTU

JCARME
ISSN: 2228-7922

Journal of Computational and Applied Research in Mechanical Engineering
Vol. 7, No. 1, pp. 85-97
jcarme.srttu.edu

LQG vibration control of sandwich beams with transversely flexible core equipped with piezoelectric patches

N. Nadirian, H. Biglari*and M. A. Hamed

[a]*Mechanical Engineering Department, University of Tabriz, Tabriz, 5166614766, Iran.*

Article info:
Received: 19/12/2015
Accepted: 25/04/2016
Online: 15/07/2017

Keywords:
Three layered sandwich theory,
Flexible core,
Active damping,
Linear quadraticregulator.

Abstract

The purpose of this paper is to control simply supported flexible core sandwich beam's linear vibration equipped with piezoelectric patches under different loads. The effects of external forces imposed on the sandwich beam can be reached to a minimum value by designing an appropriate controller and control the beam's vibration. Three-layer sandwich beam theory is used for analytical modeling of sandwich beam vibration. Euler-Bernoulli beam theory and linear displacement field are used for the face-sheets and the soft core, respectively. The piezoelectric stress resultants are expressed in terms of Heaviside discontinuity functions. Governing equations of motion are obtained using Hamilton's principle. The state space equations of the system are derived from governing equations of motion, by defining suitable state variables and using Galerkin's method. The controller is designed using linear quadratic Gaussian (LQG) technique and Kalman filter is used to estimate the state of the system. The numerical results are compared with those available in the literature. The obtained results show that the controller can play a big role toward damping out the vibration of the sandwich beam. It also shows the difference between the vibration of top face sheets and bottom face sheets because of the flexibility of the core and the situations of sensor and actuator on the top or bottom face sheets have an important role on the dynamic response of sandwich beam.

1. Introduction

In the recent years, use of smart structures consisting of composite and sandwich panel has been increased considerably due to high strength and rigidity. One of the most important reasons for using these structures is the possibility of taking advantages of piezoelectric layers. They are usually made of three parts; top and bottom face sheets, a foam or honeycomb core. Faces are generally made of high strength materials, whereas the core layer is made of a low specific weight material. So, the flexibility of the core is more than the face sheets [1]. The honeycomb cores are very flexible in all directions, compared with the face sheets. So, the in-plane stresses of the core can be neglected compared to face-sheets, whereas its transverse vibration must be considered.

Generally, two approaches are largely used to analyze sandwich structures [2]: equivalent single layer (ESL) and layer wise (LW) theories.

**Corresponding author*
Email address: hbiglari@tabrizu.ac.ir

In ESL theories, assuming the displacements in form of continuously differentiable function of thickness coordinate, the sandwich panel is analyzed as a2D equivalent single layer. In LW theories, such as three layered theories, a unique displacement field assumes for each layer in which the interface kinematic continuity conditions fulfills. Ganapathi and Makhecha [3] developed a nonlinear transient analysis of a thick sandwich plate with higher order theory. The geometric nonlinearity is introduced in the formulation based on the relevant Green's strain vector for the laminate. The governing equations of motion obtained here are solved through eigenvalue solution for free vibration case integration technique is employed for the transient response analysis. Biglari and Jafari [2] studied a closed-form solution of static problems and free vibrations of a doubly curved sandwich shell with flexible core based on three-layered high-order sandwich panel theory. Mantari and Soares [4] studied generalized layer wise HSDT and finite element formulation for symmetric laminated and sandwich composite plates for the first time.

The control of vibration is the important factor which shall be considered in designing a dynamic structure. With the new methods for decreasing vibration amplitude, active control is a reasonably applied method in which the reaction of the structure is accordance to the environmental excitation. In the active damped methods, the vibration of structures can be measured by sensors and after necessary examination by the controller, the messages will be sent to the actuators which at the end, results in depreciation of vibration.

At the early time, serious attentions have been paid to the analysis of piezoelectric beams based on approximate theories. Abramovich and Pletner [5] presented the equations of motion of new adaptive sandwich structures with piezoelectric patches in a sufficiently accurate model and in a form readily for a solution either in closed-form or by approximate methods. Hwu et al. [6] formulated the forced vibration of composite sandwich beams with piezoelectric sensors and actuators. They used modal analyze for solving the problem. An efficient new coupled zigzag theory is developed for dynamics of piezoelectric composite and sandwich beams with damping by Kapuria and Ahmed and Dumir [7]. Azrar et al. [8] analyzed active control of nonlinear vibration of sandwich piezoelectric beams. They used the Harmonic balanced method. Ramesh Kumar and Narayanan [9] considered the optimal placement of collocated piezoelectric actuator/sensor pairs on flexible beams using a model-based linear quadratic regulator (LQR) controller. A finite element method based on Euler–Bernoulli beam theory was used in their paper and they carried out the optimal location of actuator and sensor for different boundary condition. Dash and Singh [10] studied nonlinear free vibration of a piezoelectric laminated composite plate, numerically. They used Hamilton's principle and finite element method for analysis and design. Azadi et al. [11] studied an adaptive inverse dynamics control which was applied to control and suppress the micro-vibrations of a flexible panel. The piezoelectric full layers were used as sensors and actuators at the top and bottom layer. Micro-vibrations, defined as the low amplitude vibrations at the frequencies up to 1 kHz in their works. Chhabra et al. [12] considered the active vibration control of cantilever beam like structures with the laminated piezoelectric sensor and actuator layers bonded on top and bottom surfaces of the beam. A finite element model based on Euler-Bernoulli beam theory has been developed and designing of state/output feedback control by Pole placement technique and LQR optimal control approach is demonstrated to achieve the desired control. They used third order zigzag approximation for the axial displacement. The electric field was approximated as piecewise linear for the sub-layers. Moutsopoulou et al. [13] simulated and modeled smart beams with Robust Control subjected to wind induced vibration. They used first-order shear deformation theory and Galerkin's method and LQR method for vibration control.

There are few reports about vibrations control of transversely flexible core sandwich beam, using three layered theories. In this paper, vibration control of transversely flexible core sandwich beams equipped with piezoelectric patches under different loads is carried out through three layered theory. Euler-Bernoulli beam theory and linear displacement field are used for the face-sheets and the soft core, receptively.The state space equations of the system are derived from governing equations of motion, by defining suitable state variables and using Galerkin's method. The controller is designed using LQG technique and Kalman filter is used to estimate the state of the system. The numerical results are compared with those available in the literature. The obtained results show that the controller can play a big role toward damping out the vibration of the sandwich beam. It also shows the difference between the vibration of top face sheets and bottom face sheets because of the flexibility of the core.

2. Theoretical formulation

2.1. Equations of motion

A simply supported sandwich beam with a rectangular cross-section in which, one pair of piezoelectric patches is embedded symmetrically at the top and the bottom surfaces of the beam, is shown in Fig. 1. The top and bottom patches act like an actuator and a sensor, respectively. Three-layer sandwich beam theory is used for analytical modeling of sandwich beam vibration. The Euler-Bernoulli beams theory is used for top and bottom faces modeling and linear polynomial displacement field theory is used for core layer. The face-sheets and core materials are assumed to behave in a linear elastic manner. The thickness of the core is much larger than the face sheets and a perfect bonding between the face sheets and the core is postulated. The beam has length L, width b and thicknesses d_t for top face, c for core and d_b for bottom face. The piezoelectric has width b and thicknesses h_S and h_A for sensor and actuator, respectively.

Displacement field of the face-sheets and the core are as follows [14]:

$$\text{top(classic):}\quad \begin{cases} u^t(x,y,z,t) = u_0^t(x,t) \\ \qquad\qquad -(z - \dfrac{c+d_t}{2})\dfrac{\partial w^t(x,t)}{\partial x} \\ w^t(x,y,z,t) = w_0^t(x,t) \end{cases}$$

$$\text{core(linear):}\quad \begin{cases} u^c(x,y,z,t) = u_0^c(x,t) + z u_1^c(x,t) \\ w^c(x,y,z,t) = w_0^c(x,t) + z w_1^c(x,t) \end{cases}$$

$$\text{bottom(classic):}\quad \begin{cases} u^b(x,y,z,t) = u_0^b(x,t) \\ \qquad\qquad -(z + \dfrac{c+d_b}{2})\dfrac{\partial w^b(x,t)}{\partial x} \\ w^b(x,y,z,t) = w_0^b(x,t) \end{cases} \tag{1}$$

Using continuity condition between the face-sheets and the core in all directions and the weak core theory, following relations are obtained:

$$\begin{cases} u^c\big|_{z=-c/2} = u^b\big|_{z=-c/2} \\ w^c\big|_{z=-c/2} = w^b\big|_{z=-c/2} \end{cases}$$

$$\begin{cases} u^c\big|_{z=c/2} = u^t\big|_{z=c/2} \\ w^c\big|_{z=c/2} = w^t\big|_{z=c/2} \end{cases}$$

$$\text{Weak core: } \sigma_x^c = \sigma_y^c = \tau_{xy}^c = 0 \tag{2}$$

Constitutive equations of piezoelectric layers are as follows [15]:

$$\{\sigma\} = [Q]\{\varepsilon\} - [e]\{E\}$$

$$\begin{Bmatrix} \sigma_x \\ \sigma_y \\ \sigma_z \\ \tau_{yz} \\ \tau_{xz} \\ \tau_{xy} \end{Bmatrix} = \begin{bmatrix} Q_{11} & Q_{12} & Q_{13} & 0 & 0 & Q_{16} \\ Q_{21} & Q_{22} & Q_{23} & 0 & 0 & Q_{26} \\ Q_{31} & Q_{32} & Q_{33} & 0 & 0 & Q_{36} \\ 0 & 0 & 0 & Q_{44} & Q_{45} & 0 \\ 0 & 0 & 0 & Q_{54} & Q_{55} & 0 \\ Q_{61} & Q_{62} & Q_{63} & 0 & 0 & Q_{66} \end{bmatrix} \begin{Bmatrix} \varepsilon_x \\ \varepsilon_y \\ \varepsilon_z \\ \gamma_{yz} \\ \gamma_{xz} \\ \gamma_{xy} \end{Bmatrix} - \begin{bmatrix} 0 & 0 & \overline{e}_{31} \\ 0 & 0 & \overline{e}_{32} \\ 0 & 0 & \overline{e}_{33} \\ 0 & \overline{e}_{24} & 0 \\ \overline{e}_{15} & 0 & 0 \\ 0 & 0 & 0 \end{bmatrix} \begin{Bmatrix} E_x \\ E_y \\ E_z \end{Bmatrix} \tag{3}$$

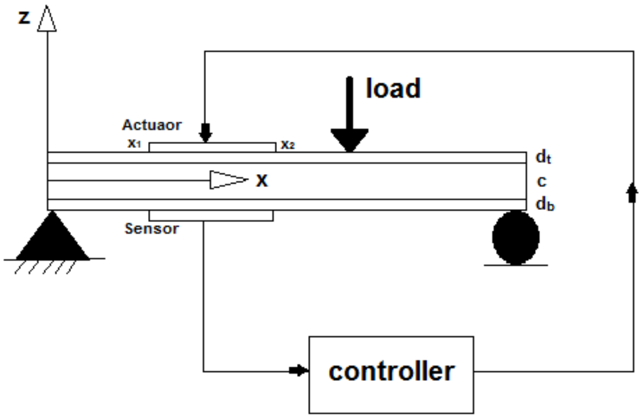

Fig. 1 Simply supported sandwich beam with piezoelectric patch.

where σ, Q, ε, E, and e are the stress, stress-reduced stiffness, strain, electric field and piezoelectric moduli matrixes, respectively. It is assumed that electric field is only in the z direction and it is constant along it [15]:

$$E_z^A = \frac{V(t)}{h_A} \tag{4}$$

where $V(t)$ is the voltage difference of the actuator piezoelectric patch surfaces. The stress fields of sandwich layers and piezoelectric sensor are only due to mechanical loading. Whereas, the stresses of actuator consist of two parts [10]: (a) mechanical components, (b) electrical components. So, the stress fields of sandwich layers, sensor and actuator are as follows:

$$\begin{aligned} \sigma_x^k &= \bar{Q}_{11}^K \varepsilon_x^K \\ \sigma_x^{actuator} &= \bar{Q}_{11}^A \varepsilon_x^A - \bar{e}_{31}^A E_z^A \\ \sigma_x^{sensor} &= \bar{Q}_{11}^S \varepsilon_x^S \end{aligned} \tag{5}$$

Equations of motion are derived according to Hamilton's principle:

$$\delta \int_{t_1}^{t_2} (-T + U + V) dt = 0 \tag{6}$$

where T, U, and V are kinetic energy, strain energy and external work done by the external forces, respectively. The strain energies of face sheets, core and piezoelectric due to bending are [16]:

$$\begin{aligned} &\delta U_{top} = \int_{V_t} \sigma_x^t \delta\varepsilon_x^t dv \\ &\delta U_{bottom} = \int_{V_b} \sigma_x^b \delta\varepsilon_x^b dv \\ &\delta U_{core} = \int_{V_c} (\sigma_z^c \delta\varepsilon_z^c + \tau_{xz}^c \delta\gamma_{xz}^c) dv \\ &\delta U_{actuator(mechanical)} = \\ &\quad \int_{V_a} \sigma_{mech}^A \delta\varepsilon_x^t (H(x-x_1) - H(x-x_2)) dv \\ &\delta U_{actuator(electrical)} = \\ &\quad \int_{V_a} \sigma_{elec}^A \delta\varepsilon_x^t (H(x-x_1) - H(x-x_2)) dv \\ &\delta U_{sensor} = \\ &\quad \int_{Vs} \sigma_x^S \delta\varepsilon_x^b (H(x-x_1) - H(x-x_2)) dv \end{aligned} \tag{7}$$

In the last equations, $H(x)$ is the unit step function. The kinetic energies of the sandwich beam and piezoelectric layers due to bending are [17]:

$$\begin{aligned} &\delta T_{top} = \int_{V_t} \rho_t (\dot{u}^t \delta\dot{u}^t + \dot{w}^t \delta\dot{w}^t) dv \\ &\delta T_{bottom} = \int_{V_b} \rho_b (\dot{u}^b \delta\dot{u}^b + \dot{w}^b \delta\dot{w}^b) dv \\ &\delta T_{core} = \int_{V_c} \rho_c (\dot{u}^c \delta\dot{u}^c + \dot{w}^c \delta\dot{w}^c) dv \\ &\delta T_{actuator} = \int_{Va} \begin{pmatrix} \rho_A (\dot{u}^t \delta\dot{u}^t + \dot{w}^t \delta\dot{w}^t) \\ \times (H(x-x_1) - H(x-x_2)) \end{pmatrix} dv \\ &\delta T_{sensor} = \int_{Vs} \begin{pmatrix} \rho_s (\dot{u}^b \delta\dot{u}^b + \dot{w}^b \delta\dot{w}^b) \\ \times (H(x-x_1) - H(x-x_2)) \end{pmatrix} dv \end{aligned} \tag{8}$$

It is assumed that the transverse external force is applied only to the top layer of the sandwich beam in the z direction. So, the potential energy due to the external work is [2, 16]:

$$\delta V = -\int_0^b \int_0^l F(x,t)\delta w_0^t dxdy \tag{9}$$

Now, by substitution the Eqs. (7-9) to the Hamilton principle and using constitutive relations Eq. (3), the equations of motions are derived as:

δu_0^t :

$$\begin{aligned}
&\left(I_1^t + I_1^A H + \frac{I_1^c}{4} + \frac{I_3^c}{c^2}\right)\ddot{u}_0^t + \left(\frac{I_1^c}{4} - \frac{I_3^c}{c^2}\right)\ddot{u}_0^b \\
&-\left(I_2^t + I_2^A H - \frac{d_t}{2}\left(\frac{I_1^c}{4} + \frac{I_3^c}{c^2}\right)\right)\frac{\partial \ddot{w}_0^t}{\partial x} - \frac{d_b}{2}\left(\frac{I_1^c}{4} - \frac{I_3^c}{c^2}\right)\frac{\partial \ddot{w}^b}{\partial x} \\
&-\frac{\partial N_x^t}{\partial x} - Q_{11}^A H_1^A\left(H'\frac{\partial u_0^t}{\partial x} + H\frac{\partial^2 u_0^t}{\partial x^2}\right) \\
&+Q_{11}^A H_2^A\left(H'\frac{\partial^2 w_0^t}{\partial x^2} + H\frac{\partial^3 w_0^t}{\partial x^3}\right) + \frac{Q_x^c}{c} + e_{31}^A E_z^A H_1^A H' = 0
\end{aligned} \tag{10.a}$$

δw_0^t :

$$\begin{aligned}
&I_2^A H'\ddot{u}_0^t - I_3^A H'\frac{\partial \ddot{w}_0^t}{\partial x} + \left(\frac{I_1^c}{4} - \frac{I_3^c}{c^2}\right)\ddot{w}_0^b \\
&+\left(I_2^t + I_2^A H - \frac{d_t}{2}\left(\frac{I_1^c}{4} + \frac{I_3^c}{c^2}\right)\right)\frac{\partial \ddot{u}_0^t}{\partial x} \\
&+\frac{d_t}{2}\left(\frac{I_1^c}{4} - \frac{I_3^c}{c^2}\right)\frac{\partial \ddot{u}_0^b}{\partial x} \\
&+\left(I_1^t + I_1^A H + \frac{I_1^c}{4} + \frac{I_3^c}{c^2}\right)\ddot{w}_0^t \\
&-\left(I_3^t + I_3^A H + \frac{d_t^2}{4}\left(\frac{I_1^c}{4} + \frac{I_3^c}{c^2}\right)\right)\frac{\partial^2 \ddot{w}_0^t}{\partial x^2} \\
&+\frac{d_t d_b}{4}\left(\frac{I_1^c}{4} - \frac{I_3^c}{c^2}\right)\frac{\partial^2 \ddot{w}^b}{\partial x^2} - \frac{\partial^2 M_x^t}{\partial x^2} + \frac{N_z^c}{c} \\
&-Q_{11}^A H_2^A\left(\begin{array}{l} H''\dfrac{\partial u_0^t}{\partial x} + 2H'\dfrac{\partial^2 u_0^t}{\partial x^2} \\ +H\dfrac{\partial^3 u_0^t}{\partial x^3}\end{array}\right) \\
&+Q_{11}^A H_3^A\left(\begin{array}{l} H''\dfrac{\partial^2 w_0^t}{\partial x^2} + 2H'\dfrac{\partial^3 w_0^t}{\partial x^3} \\ +H\dfrac{\partial^4 w_0^t}{\partial x^4}\end{array}\right) \\
&-\left(\frac{d_t}{2c} + \frac{1}{2}\right)\frac{\partial Q_x^c}{\partial x} - \frac{1}{c}\frac{\partial S_x^c}{\partial x} \\
&+e_{31}^A E_z^A H_2^A H'' = F_t(x,t)
\end{aligned} \tag{10.b}$$

δu_0^b :

$$\begin{aligned}
&\left(\frac{I_1^c}{4} - \frac{I_3^c}{c^2}\right)\ddot{u}_0^t + \left(I_1^b + I_1^S H + \frac{I_1^c}{4} + \frac{I_3^c}{c^2}\right)\ddot{u}_0^b \\
&+\frac{d_t}{2}\left(\frac{I_1^c}{4} - \frac{I_3^c}{c^2}\right)\frac{\partial \ddot{w}^t}{\partial x} \\
&-\left(I_2^b + I_2^S H + \frac{d_b}{2}\left(\frac{I_1^c}{4} + \frac{I_3^c}{c^2}\right)\right)\frac{\partial \ddot{w}_0^b}{\partial x} \\
&-\frac{\partial N_x^b}{\partial x} - Q_{11}^S H_1^S\left(H'\frac{\partial u_0^b}{\partial x} + H\frac{\partial^2 u_0^b}{\partial x^2}\right) \\
&+Q_{11}^S H_2^S\left(H'\frac{\partial^2 w_0^b}{\partial x^2} + H\frac{\partial^3 w_0^b}{\partial x^3}\right) - \frac{Q_x^c}{c} = 0
\end{aligned} \tag{10.c}$$

δw_0^b :

$$\begin{aligned}
&\frac{d_b}{2}\left(\frac{I_1^c}{4} - \frac{I_3^c}{c^2}\right)\frac{\partial \ddot{u}_0^t}{\partial x} + \left(\frac{I_1^c}{4} - \frac{I_3^c}{c^2}\right)\ddot{w}_0^t + I_2^S H'\ddot{u}_0^b \\
&+\frac{d_t d_b}{4}\left(\frac{I_1^c}{4} - \frac{I_3^c}{c^2}\right)\frac{\partial^2 \ddot{w}^t}{\partial x^2} - I_3^S H'\frac{\partial \ddot{w}_0^b}{\partial x} \\
&+\left(I_2^b + I_2^S H + \frac{d_b}{2}\left(\frac{I_1^c}{4} + \frac{I_3^c}{c^2}\right)\right)\frac{\partial \ddot{u}_0^b}{\partial x} \\
&+\left(I_1^b + I_1^S H + \frac{I_1^c}{4} + \frac{I_3^c}{c^2}\right)\ddot{w}_0^b \\
&-\left(I_3^b + I_3^S H + \frac{d_b^2}{4}\left(\frac{I_1^c}{4} + \frac{I_3^c}{c^2}\right)\right)\frac{\partial^2 \ddot{w}_0^b}{\partial x^2} \\
&-\frac{\partial^2 M_x^b}{\partial x^2} - \frac{N_z^c}{c} - \left(\frac{d_t}{2c} + \frac{1}{2}\right)\frac{\partial Q_x^c}{\partial x} + \frac{1}{c}\frac{\partial S_x^c}{\partial x} \\
&-Q_{11}^S H_2^S\left(H''\frac{\partial u_0^b}{\partial x} + 2H'\frac{\partial^2 u_0^b}{\partial x^2} + H\frac{\partial^3 u_0^b}{\partial x^3}\right) \\
&+Q_{11}^S H_3^S\left(H''\frac{\partial^2 w_0^b}{\partial x^2} + 2H'\frac{\partial^3 w_0^b}{\partial x^3} + H\frac{\partial^4 w_0^b}{\partial x^4}\right) = 0
\end{aligned} \tag{10.d}$$

In the above relations, the stress resultants are:

$$\begin{aligned}
&\left\{N_x^t, M_x^t\right\} = \sum\int_{z_l}^{z_{l+1}} \sigma_x^t (1, z - \frac{c+d_t}{2})dz \\
&\left\{N_x^b, M_x^b\right\} = \sum\int_{z_l}^{z_{l+1}} \sigma_x^b (1, z + \frac{c+d_b}{2})dz \\
&N_z^c = \int_{-\frac{c}{2}}^{\frac{c}{2}} \sigma_z^c dz, Q_x^c = \int_{-\frac{c}{2}}^{\frac{c}{2}} K\tau_{xz}^c dz \\
&S_x^c = \int_{-\frac{c}{2}}^{\frac{c}{2}} Kz\tau_{xz}^c dz, Q_x^{*c} = \int_{-\frac{c}{2}}^{\frac{c}{2}} K\tau_{xz}^c z^2 dz
\end{aligned} \tag{11}$$

The constant and inertia terms are as follows:

$$\begin{aligned}
&H_i^A = \frac{b}{i}\left[(\frac{c}{2} + d_t + h_A - \frac{c+d_t}{2})^i - (\frac{c}{2} + d_t - \frac{c+d_t}{2})^i \right] \\
&H_i^S = \frac{b}{i}\left[(-\frac{c}{2} - d_b + \frac{c+d_b}{2})^i - (-\frac{c}{2} - d_b - h_S + \frac{c+d_b}{2})^i \right] \\
&I_i^c = \int_{-\frac{c}{2}}^{\frac{c}{2}} b\rho_c z^i dz
\end{aligned} \tag{12}$$

$$I_i^t = \sum_{L=1}^{N_t} \int_{Z_L}^{Z_{L+1}} b\rho_L^t \left(z - \frac{c+d_t}{2} \right)^i dz$$
$$I_i^b = \sum_{L=1}^{N_b} \int_{Z_L}^{Z_{L+1}} b\rho_L^b \left(z + \frac{c+d_b}{2} \right)^i dz$$
$$I_i^A = \sum \int_{\frac{c}{2}+d_t}^{\frac{c}{2}+d_t+h_A} b\rho_l^A \left(z - \frac{c+d_t}{2} \right)^i dz$$
$$I_i^S = \sum \int_{-\frac{c}{2}-d_b-h_S}^{-\frac{c}{2}-d_b} b\rho_l^S \left(z + \frac{c+d_b}{2} \right)^i dz$$

By substituting Eqs. (11 and 12) in Eqs. (10), the governing equations of motion based on displacement are achieved.

2.2. Solution procedure

In this section, Galerkin's method is used to discretize the set of partial differential equations of the beam. For most structural systems under practical loading conditions, the forced vibration response is mainly due to a contribution from the first few natural modes. In this section, mode superposition method is adopted to obtain an approximate reduced-order dynamic model of the system in the time domain. The mode shapes of the simply supported sandwich beam are as follows:

$$\begin{cases} u_0^t(x,t) = \sum_{m=1}^{M} U_m^t(t)\cos(\alpha_m x) \\ w_0^t(x,t) = \sum_{m=1}^{M} W_m^t(t)\sin(\alpha_m x) \\ u_0^b(x,t) = \sum_{m=1}^{M} U_m^b(t)\cos(\alpha_m x) \\ w_0^b(x,t) = \sum_{m=1}^{M} W_m^b(t)\sin(\alpha_m x) \end{cases} \tag{13}$$

where $U_m^t(t), W_m^t(t), U_m^b(t)$ *and* $W_m^b(t)$ are generalized coordinates and $\cos(\alpha_m x), \sin(\alpha_m x)$ is the comparison function. By substituting Eq. (13) in Eq. (10) and multiplying the relations (10.a) and (10.c) by function $\cos(\alpha_m x)$ and relations (10.b) and (10.d) by function $\sin(\alpha_m x)$, integrating over the length of the beam, and using the modes orthogonally principle, we obtain Eq. (14) in time domain:

$$\begin{gathered} [\mathbf{M}]\ddot{\mathbf{Z}} + [\mathbf{K}]\mathbf{Z} = \mathbf{F}_\mathrm{v}V(t) + \mathbf{F}_\mathrm{f}F(t) \\ \mathbf{Z} = \{U_m^t, W_m^t, U_m^b, W_m^b\}^T \end{gathered} \tag{14}$$

where **M** and **K** are the generalized mass and stiffness matrices, V is voltage, F is external load, $\mathbf{F_f}$ is the vector external load coefficient and $\mathbf{F_v}$ the generalized control force vector produced by electromechanical coupling effects. Eq. (14) can be expressed in state space form as:

$$\begin{cases} \dot{\mathbf{x}} = \mathbf{A}\mathbf{x} + \mathbf{B}_\mathrm{f}F(t) + \mathbf{B}_\mathrm{v}V(t) \\ \mathbf{Y} = \mathbf{C}\mathbf{x} + \mathbf{D}_\mathrm{f}F(t) + \mathbf{D}_\mathrm{v}V(t) \end{cases}, \mathbf{x} = \begin{Bmatrix} \mathbf{Z} \\ \dot{\mathbf{Z}} \end{Bmatrix} \tag{15}$$

where, **A** is system matrix, $\mathbf{B}_v$ is control matrix, $\mathbf{B}_f$ is disturbance matrix, $F(t)$ is the disturbance input and $V(t)$ is is the control input to the actuator. The matrixes **A**, $\mathbf{B}_f$ and $\mathbf{B}_v$ are as follows:

$$\begin{gathered} \mathbf{A} = \begin{bmatrix} \mathbf{0}_{(4m\times 4m)} & \mathbf{I}_{(4m\times 4m)} \\ \left[(-\mathbf{M}^{-1}\mathbf{K})\right]_{(4m\times 4m)} & \mathbf{0}_{(4m\times 4m)} \end{bmatrix}_{(8m\times 8m)}, \\ \mathbf{B}_f = \begin{bmatrix} \mathbf{0}_{(4m\times 1)} \\ \left[(\mathbf{M}^{-1}\mathbf{F}_f)\right]_{(4m\times 1)} \end{bmatrix}_{(8m\times 1)}, \\ \mathbf{B}_v = \begin{bmatrix} \mathbf{0}_{(4m\times 1)} \\ \left[(\mathbf{M}^{-1}\mathbf{F}_v)\right]_{(4m\times 1)} \end{bmatrix}_{(8m\times 1)} \end{gathered} \tag{16}$$

For controlling purposes, the output of system is the vibration (displacement) of beam at x_c (middle of the beam):

$$\mathbf{Y} = \mathbf{C} \begin{Bmatrix} \sum_{m=1}^{M} U_m^t(t)\cos(\alpha_m x_c) \\ \sum_{m=1}^{M} W_m^t(t)\sin(\alpha_m x_c) \\ \sum_{m=1}^{M} U_m^b(t)\cos(\alpha_m x_c) \\ \sum_{m=1}^{M} W_m^b(t)\sin(\alpha_m x_c) \end{Bmatrix}, \tag{17}$$

$$\mathbf{C}=\begin{bmatrix}\begin{bmatrix}\cos(\alpha_m x_c)\ 0\ 0\ 0\\ 0\ \sin(\alpha_m x_c)\ 0\ 0\\ 0\ 0\ \cos(\alpha_m x_c)\ 0\\ 0\ 0\ 0\ \sin(\alpha_m x_c)\end{bmatrix} & \mathbf{0}_{(4\times 4m)}\end{bmatrix},$$

$$\mathbf{D_f}=\begin{bmatrix}0\\0\\0\\0\end{bmatrix},\quad \mathbf{D_v}=\begin{bmatrix}0\\0\\0\\0\end{bmatrix}$$

2.3. Control law

Linear quadratic regulator (LQR) is an optimal control procedure, in which energy-like criteria are used and the minimization procedure automatically produces controllers that are stable and somewhat robust. The key idea is to design an optimal control to minimize a cost function or a performance index which is a quadratic function of the desired system response and required control force [18]:

$$J=\int_0^\infty (\mathbf{X}^T\mathbf{Q}\mathbf{X}+\mathbf{V}^T\mathbf{R}\mathbf{V})dt \tag{18}$$

where Q and R are semi-positive-definite and positive definite weighting matrices on the outputs and control inputs, respectively.
Assuming full state feedback, the control law is given by:

$$\mathbf{V}(t)=-\mathbf{K}_{LQR}^T\mathbf{x}(t) \tag{19}$$

By substituting eq. (19) in eq. (15):

$$\begin{cases}\dot{\mathbf{x}}=(\mathbf{A}-\mathbf{B_v}\mathbf{K}_{LQR}^T)\mathbf{x}+\mathbf{B_f}F(t)\\ \mathbf{Y}=\mathbf{C}\mathbf{x}+\mathbf{D_f}F(t)+\mathbf{D_v}V(t)\end{cases} \tag{20}$$

According to eq. (19), measuring all state variables is not possible. But, it is necessary to measure system output, which is the sensor output voltage. So, the system may be used to estimate of the state vector. Kalman filter is used to estimate the state of the system. Sensor layer output voltage is considered as system output **y**. Using relations introduced in section 4 of reference [15], it can be easily shown that $\mathbf{y}=C_{sensor}\mathbf{x}$, where parameter **x** is the state vector.

Based on this assumption, Kalman filter formulation is as follow [18]:

$$\begin{cases}\dot{\hat{x}}=A\hat{x}+B_vV(t)+L_e(y-\hat{y}_{sensor})\\ y=V_{sensor}\quad,\quad \hat{y}_{sensor}=C_{sensor}\hat{x}\end{cases} \tag{21}$$

where L_e is the Kalman gain. By using LQR and Kalman filter, simultaneously, LQG method is obtained as follow:

$$\begin{cases}V(t)=V_{actuator}=-K_{LQR}^T\hat{x}\\ \dot{x}=(A-B_vK_{LQR}^T-L_eC_{sensor})\hat{x}+(L_eC_{sensor})x\end{cases} \tag{22}$$

3. Results and discussion

In order to examine the accuracy of the present structural formulation, the response of a sandwich beam with flexible core and simply supported boundary condition to step load obtained from the proposed method are compared with those available in the literature [14]. After validating the presented model, to assess the performance of the piezoelectric patches in controlling the responses of sandwich beams under different load, extensive numerical results are presented.

3.1. Comparative study

First, the response of sandwich beam to dynamic step load (0.5 kN/m) obtained from the presentmethod are compared with those reported by Hamed and Rabinovitch [14] for sandwich beams with a flexible core. The materialproperties are presented in Table 1.
In Fig. 2, the nondimensional transverse vibration (w_{dynmic}/w_{static}) of the middle point of bottom face sheet is illustrated. It can be seen from Fig. 2 that the present solution matches very well with the results obtained by Hamed and Rabinovitch [14]. Thus, the correctness of the present formulations is demonstrated.

3.2. New result

In this section, new results for vibration control of smart sandwich beam with flexible core and simply supported boundary conditions are presented. A sandwich beam equipped with one actuator and one sensor was bonded symmetrically on the surfaces of the sandwich beam. The geometry and mechanical properties are presented in Table 1. The piezoelectric patches are PZT-5H [19].

In the following, comparison of controlled and uncontrolled vibration of the beam and the effects of the transverse elastic module and shear module of the core and length and position of the piezoelectric patches on the controlled vibration of the sandwich beam are investigated.

Figures 3 and 4 show comparison of controlled and uncontrolled transverse vibration of the beam under dynamic loads. Figure 3 shows the impulse loaded response of system based on the first four mode shapes of Galerkin's method. The point impulse force (-20 kN in 0.1 mili second) is applied at $l/4$ in the z direction, vibration measured at $l/2$ of sandwich beam's length, the position of patches are at $x_1=l/5$, $x_2=2l/5$ and controller parameters are **Q**=**I** (unit matrix), **R**=10^{-4}.

Figure 4 shows the uniform step loaded response of system based on the first four mode shapes of Galerkin's method. The uniform step force (800 N/m) is applied at the full length of the beam, vibration measured at $l/2$ of sandwich beam's length, the position of the patch are at $x_1=l/5$, $x_2=2l/5$ and controller parameters are**Q**=**I** (unit matrix), **R**=10^{-5}.

According to the figures, results show that the amplitudes of displacement vibration decay in time toward zero with a controller, in both impulse point and uniform step loads. It is also shown that the transverse deflections of the upper and lower face sheets are almost identical through the entire time domain. But, axial vibrations of the top and bottom face sheets are not identical. It will be shown that the core with transverse elastic and shear modules mentioned in Table 1, has rigid flexural and flexible shearing behavior in vibration.

Table 1. Material properties [14]

	E,G GPa	*ρ* kgm^{-3}	*L* mm	*h* mm	*b* mm	e_{31} cm^{-2}
Top	18	2000	1200	6	100	-
Core	0.056,0.022	60	1200	60	100	-
Bottom	18	2000	1200	6	100	-
Actuator	60	7500	240	0.5	100	-16.604
Sensor	60	7500	240	0.0028	100	-16.604

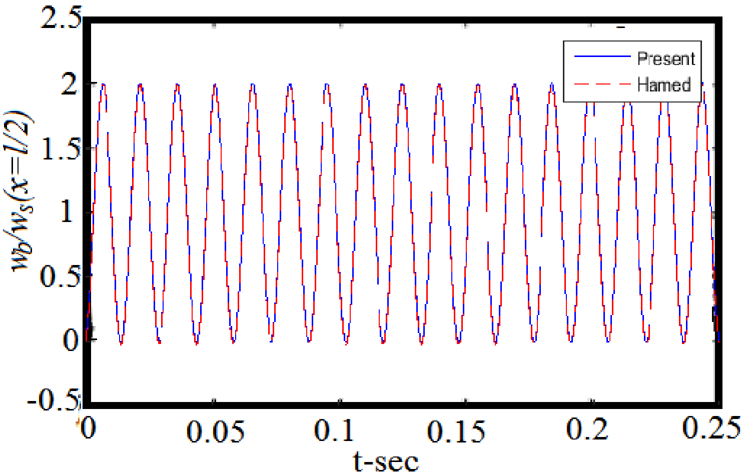

Fig. 2 The comparison of the present solutions with those from literature [14]

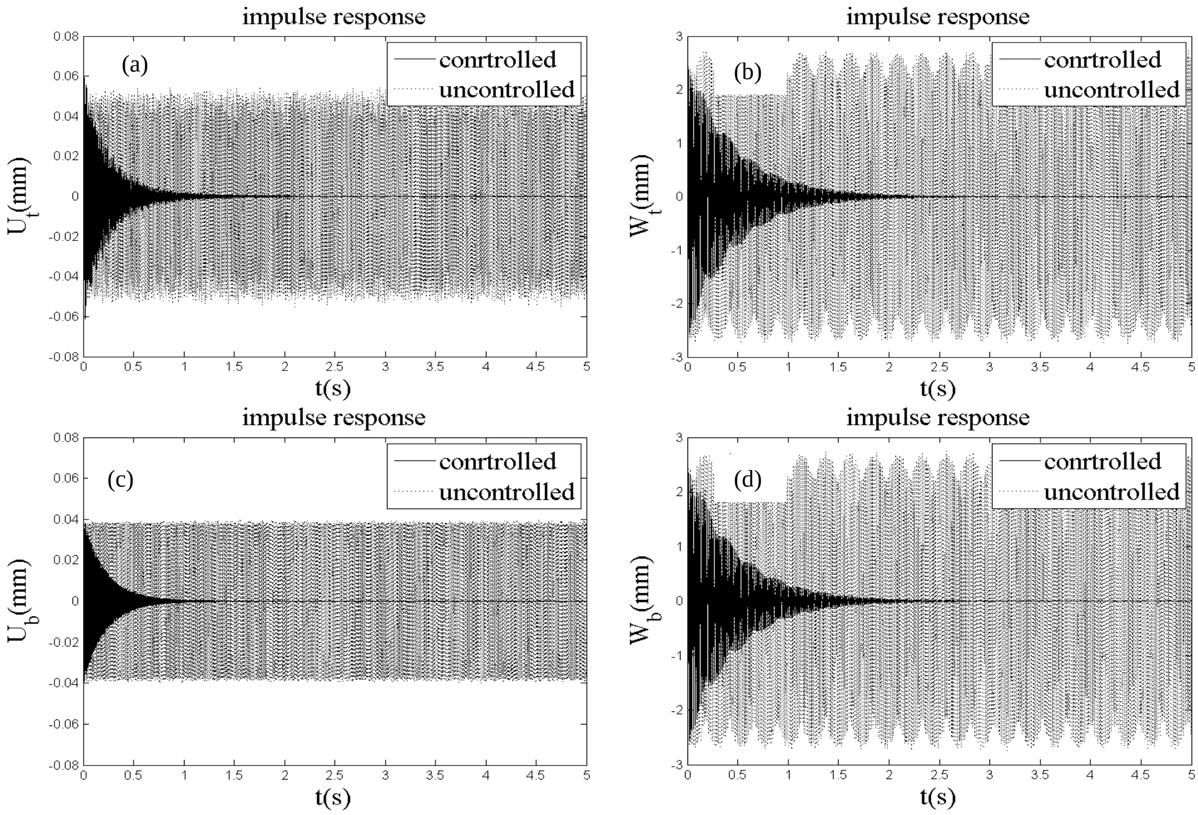

Fig. 3. Controlled and uncontrolled response of top and bottom face-sheets under point impulse load; (a) top axial, (b) top transverse, (c) bottom axial, and (d) bottom transverse displacements

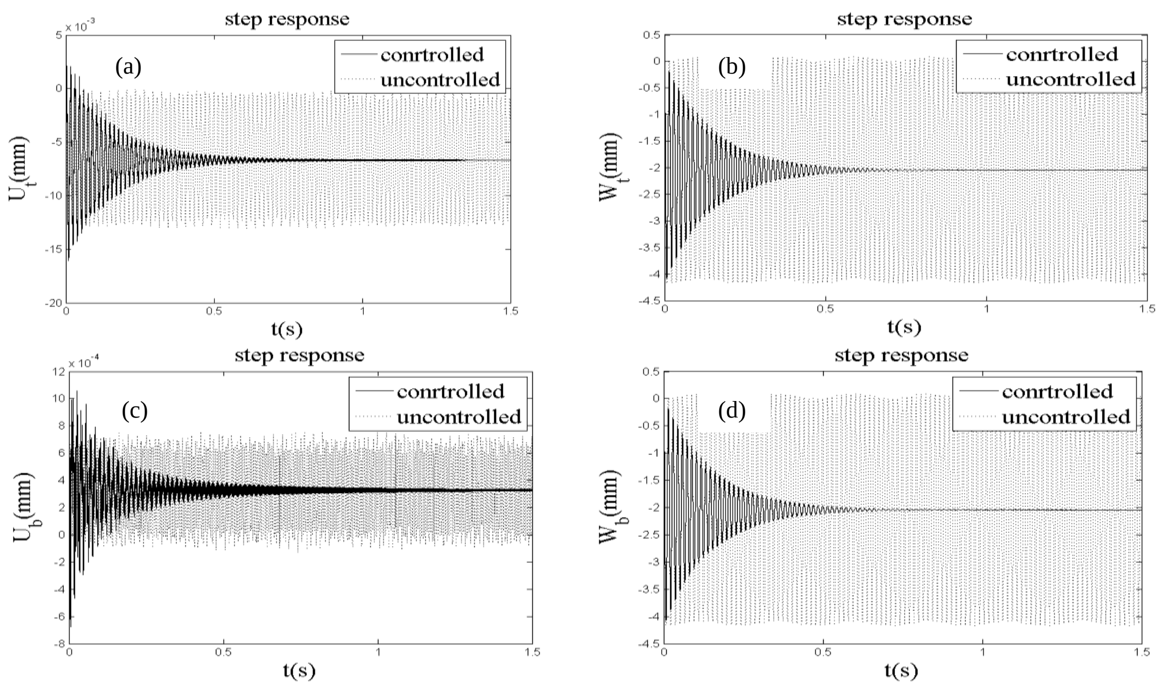

Fig. 4. Controlled and uncontrolled response of top and bottom face-sheets under uniform step load; (a) top axial, (b) top transverse, (c) bottom axial, and (d) bottom transverse displacements

The flexibility of the core conduces the difference between top and bottom face sheets displacements. This effect is associated with a change in the transverse elastic and shear modules of the core. For better consideration, effects of the transverse elastic and shear modules of the core on the force vibration of axial and transverse displacements of the top and bottom face sheets are considered in Figs. 5 and 6, separately.

In Fig. 5, the shear modulus is constant, but the elastic modulus of the core decreases (E_c=56×10^3 Pa, G_c=22×10^6 Pa). Conversely, in Fig. 6, the transverse elastic modulus is constant and the shear modulus of the core decreases (E_c=56×10^6 Pa, G_c=20×10^6 Pa).

The results of Fig. 5 show that the transverse displacement of top face in the *z* direction is larger than deflection of bottom face sheet, because of the flexural flexibility of the core. It is interesting that the results of Fig. 6 show the same deflections for both top and bottom face sheets deflection. As shown in Fig. 6, the axial displacement of the top face is much bigger than the axial displacement of bottom face sheet, because of the shearing flexibility of the core.

The competence of proposed smart sandwich beam for damping of force vibration is demonstrated in Figs. 7 and 8. Figure 7 shows the damping ratio for top face sheet deflection (W_t) in order to show the effect of patch length on the vibration controlling (damping). The damping ratio of the vibration amplitude is calculated as follow:

$$\zeta = \frac{1}{2\pi n}\ln\left(\frac{A_1}{A_{n+1}}\right) \tag{23}$$

where A_1 and A_{n+1} are the amplitudes of the first and n+1 cycle, respectively.

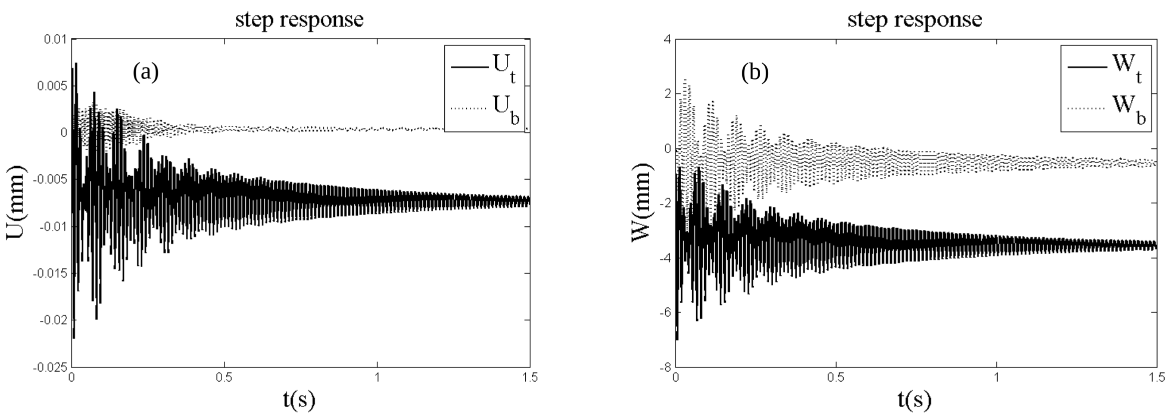

Fig. 5. Effect of elastic modulus of core on the controlled response of top and bottom face-sheets under uniform step load (E_c=56×10^{3}Pa, G_c=22×10^{6}Pa); (a) axial, and (b) transverse displacements.

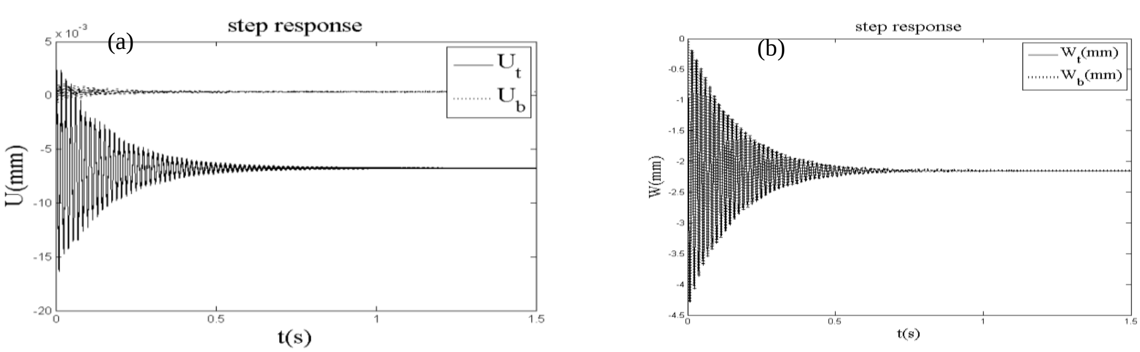

Fig. 6. Effect of shear modulus of core on the controlled response of top and bottom face-sheets under uniform step load (E_c=56×10^{6}Pa, G_c=20×10^{6}Pa); (a) axial, and (b) transverse displacements.

In Fig. 7, the piezoelectric patch is located at $x_1=l/5$ and has various lengths of $l/20$, $l/10$, and $l/5$. The sandwich beam is under impulse point load (-20 kN in z direction at the middle of the beam) and vibration is measured at $l/4$. It is seen from the figure that longer patches have greater damping ratio.

Figure 8 shows the effect of patch locations on the damping ratio. The length of the patch is constant ($l/5$) andits position locates at $x_1=0$, $l/5$, and $2l/5$. It is obvious that for symmetric boundary conditions of the beam, patches located at the same position of the beginning and end of the beam have same effects on controlling. As seen from the figure, the patch located at the middle of the beam has greater damping ratio.In addition, it is seen in Figs. 7 and 8 that increasing control weighted factor (***R***) decreases the damping ratio.

4. Conclusions

The present study is concerned with active control of dynamic response of smart sandwich beams with flexible core subjected to different loads (like impulse and uniform step loads) using piezoelectric sensor/actuator patches. Euler-Bernoulli beam theory is used for face-sheets and linear polynomial displacement field theory is used for the core. Governing equations and solution procedure of vibration are obtained using Hamilton's principle and Galerkin's method. Linear Quadratic Regulator feedback control law is applied in a closed loop system to provide active vibration control of the sandwich beam.

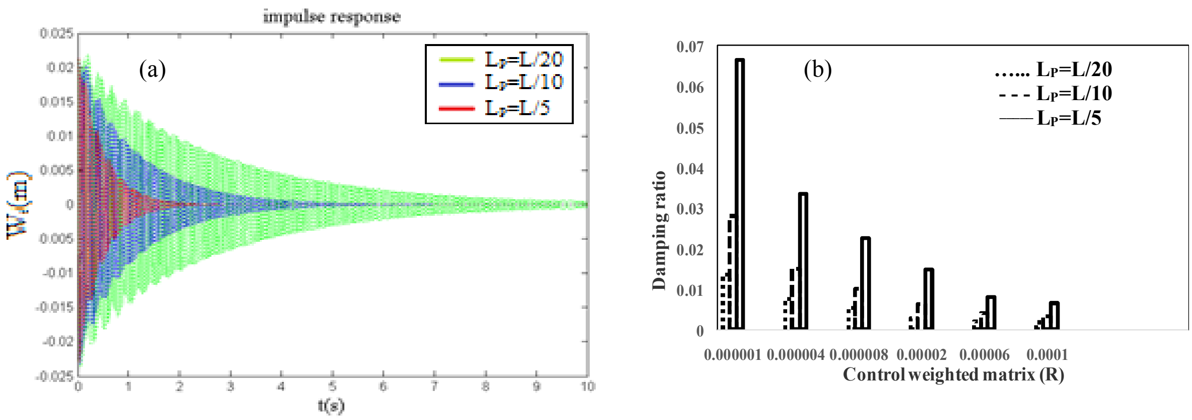

Fig. 7. Effect of patch length for impulse point load on (a) deflection vibration W_t and (b) damping ratio.

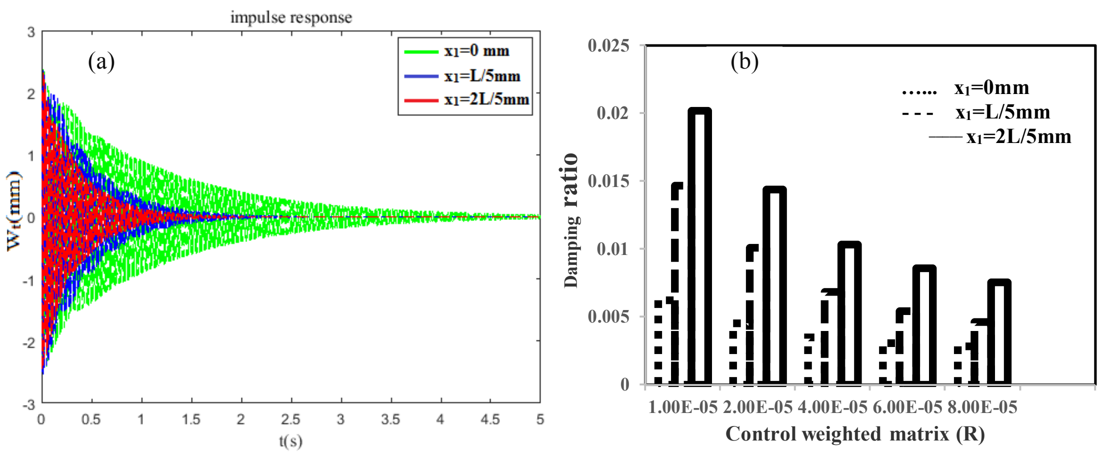

Fig. 8. Effect of patch location for impulse point load on (a) deflection vibration W_t and (b) damping ratio.

A set of the parametric study is carried out to show the effect of core flexibility, control weighted matrix, piezoelectric patch location and length of the dynamic response of sandwich beam. The obtained results reveal that the active vibration control strategy can play a big role toward damping out the vibration of the sandwich beam exposed to different loadings. The flexibility of the core conduces the difference between the top and bottom face sheets displacements that must be accounted in the design of the controller. This effect is associated with a change in the elastic modulus and shear modulus of the core. The decreasing of transverse elastic module causes decreasing of the flexural flexibility of sandwich beam and increasing of the difference between the top and bottom deflection vibration. Decreasing the shear module causes the shearing flexibility of sandwich beam to decrease, and the difference between the top and bottom axial displacement vibration to increase.

References

[1] L. Librescu, and T. Hause, "Recent developments in the modeling and behavior of advanced sandwich constructions: a survey," *Composite Structures*, Vol. 48, pp. 1-17, (2000).

[2] H. Biglari,and A. Jafari, "Static and free vibration analyses of doubly curved composite sandwich panels with soft core based on a new three-layered mixed theory," *Composite Structures*, Vol. 92, pp. 2684-2694, (2010).

[3] M. Ganapathi, B.P. Patel, and D.P. Makhecha, "Nonlinear dynamic analysis of thick composite/sandwich laminates using an accurate higher-order theory," *Composites Part B: Engineering*, Vol. 35, No. 4, pp. 345-355, (2004).

[4] J. L. Mantari, and C. Guedes Soares, "Generalized layerwise HSDT and finite element formulation for symmetric laminated and sandwich composite plates," *Composite Structures*, Vol. 105, pp. 319-331, (2013).

[5] H. Abramovich, and B. Pletner, "Actuation and sensing of piezolaminated sandwich type structures," *Composite Structure*, Vol. 38, No.1–4, 17-27, (1997).

[6] W. C. H. C. Chang, and S. S. Gai, "Forced vibration of composite sandwich beams with piezoelectric sensors and actuators," *4th Pacific International Conference on Aerospace Science and Technology*, Kaohsiung, Taiwan, 21-23, (2001).

[7] S. Kapuria, A. Ahmed, and P. C. Dumir, "An efficient coupled zigzag theory for dynamic analysis of piezoelectric composite and sandwich beams with damping," *Journal of Sound and Vibration*, Vol. 279, No. 1–2, pp. 345-371, (2005).

[8] L. Azrar, S. Belouettar, and J. Wauer, "Nonlinear vibration analysis of actively loaded sandwich piezoelectric beams with geometric imperfection," *Computers and structures*, Vol. 86, No. 2, pp. 2191-182, (2008).

[9] K. Ramesh Kumar, and S. Narayanan, "Active vibration control of beams with optimal placement of piezoelectric sensor/actuator pairs," *Smart Materials and Structures*, Vol. 17, No. 5, pp. 1-15, (2008).

[10] P. Dash, and B. N. Singh, "Nonlinear free vibration of piezoelectric laminated composite plate," *Finite Elements in Analysis and Design*, Vol. 45, No. 10, pp. 686-694, (2009).

[11] M. Azadi, E. Azadi, and M. Roopaei, "Adaptive inverse dynamics control for vibration suppression," *World Applied Sciences Journal*, Vol. 12, No. 12, pp. 2343-2351, (2011).

[12] D. Chhabra, P. Chandna, and G. Bhushan, "Design and analysis of smart structures for active vibration control using piezo-crystals," *International Journal of Engineering and Technology*, Vol. 1, No. 3, pp. 153-162 , (2011).

[13] A. Moutsopoulou, G. Stavroulakis, and T. Pouliezos. "Simulation and modelling of smart beams with robust control subjected to wind induced vibration," *Open Journal*

of Civil Engineering, Vol. 2, No. 3, pp. 106-114, (2011).

[14] E. Hamed, and O. Rabinovitch, “Modeling and dynamics of sandwich beams with a viscoelastic soft core,” *AIAA Journal*, Vol. 47, No. 9, pp. 2194-2211, (2009).

[15] J. N. Reddy, “On laminated composite plates with integrated sensors and actuators,” *Engineering Structures*, Vol. 21, No. 7, pp. 568-593, (1999).

[16] E. Padoin, O. Menuzzi, E. A. Perondi, and J. Ono Fonseca, ”Modeling and LQR/LQG control of a cantilever beam using piezoelectric material”, *22nd International congress of mechanical engineering-COBEM 2013, Ribeirão Preto, SP, Brazil.* November 3-7, (2013).

[17] Y. M. Huang, and T. J. Chen,” Passive piezoelectric absorbers on supperessing vibration of a rotating beam”, *Twelfth International Congress on Sound and Vibration*, (2005).

[18] B. D. O. Anderson, and J. B. Moore, "Optimal Control, Linear Quadratic Methods," *Prentice-Hall Inc*., New Jersey, (1989).

[19] A. R. Damanpack, M. Bodaghi, M. M. Aghdam, and M. Shakeri, ”Active control of geometrically non-linear transient response of sandwich beams with a flexible core using piezoelectric patches", *Composite Structures*, Vol. 100, pp. 517–531, (2013).

How to cite this paper:

N. Nadirian, H. Biglari and M. A. Hamed, “LQG vibration control of sandwich beams with transversely flexible core equipped with piezoelectric patches”, Journal of Computational and Applied Research in Mechanical Engineering, Vol. 7. No. 1, pp. 85-97

DOI: 10.22061/JCARME.2017.643
URL: http://jcarme.srttu.edu/article_643.html